Accurate dicrotic notch detection using adaptive shear transforms

Joel Balmer * Christopher Pretty * Alexander Amies *
Thomas Desaive ** J. Geoffrey Chase *

* Department of Mechanical Engineering, University of Canterbury,
New Zealand (email: joel.balmer@pg.canterbury.ac.nz).
** GIGA Cardiovascular Science, University of Liège, Liège, Belgium
(email: tdesaive@ulg.ac.be)

Abstract: Dicrotic notch detection in aortic pressure waveforms enables a reference in time, marking the transition from systole to diastole. Identification of the notch is useful in applications studying events specific to systole or diastole, for example, models that estimate cardiac function, and systolic time intervals such as left ventricular ejection time. The purpose of this study was to test a new dicrotic notch detection algorithm, against an existing end systole estimation method. The new algorithm utilises a shear transform, which is adaptive based on the shape of the aortic pressure waveform. To assess the accuracy of the two algorithms, 80 beats aortic pressure waveforms were used from four porcine pigs. The pigs were subjected to hemodynamic modification in order to test the algorithms on different waveforms shapes. The dicrotic notches were first found by eye in the 80 beats waveforms, and systolic time, from the start of the beat to the dicrotic notch, was the metric used to compare the accuracy of dicrotic notch locations. The new algorithm identifies features of the dicrotic notch when it is present and estimates the location when it is less clear, better than the existing method of end systole estimation. This result was evident in the mean difference between measured and estimated systolic times of 0.5ms vs 11.6ms, for the new algorithm and existing respectively. The new method also showed significantly less variation in its estimate than the existing method, across all pigs' hemodynamic states.

Keywords: Biomedical systems, Bio-signals analysis and interpretation, Dicrotic notch, End systole, Start diastole, Cardiovascular system.

1. INTRODUCTION

The dicrotic notch is a distinct stationary point in proximal arterial (often aortic) pressure signals, following the maximum pressure in a beat waveform. It may be a point of inflection with (approximately) zero gradient, or a combination of two turning points with respective local minimum and maximum.

The dicrotic notch is formed by the reflection of a wave off of the aortic valve, following valve closure (Lewis, 1906). Thus, it is clearest in proximal pressure signals and crucial for determining transition from systole to diastole in aortic pressure waveforms (Oppenheim and Sittig, 1995). Specifically, aortic systolic time, associated with left ventricular ejection, lasts from the *foot* of the aortic pressure wave to the dicrotic notch (Talley et al., 1971; Payne, 2006; Marik, 2013). Diastolic time, associated with aortic relaxation, is the remaining time from the dicrotic notch to the next pressure waveform foot.

Given the notches physical significance as a systolic/diastolic time reference, it has been used in numerous applications (e.g. pulse wave velocity calculations (Hermeling et al., 2009), models estimating cardiovascular function (Stevenson et al., 2010, 2012b), and left ventricular ejection time).

Kamoi et al. (2017) presented a pressure contour analysis method to estimate stroke volume. It is sensitive to the identification of end systole, and thus the dicrotic notch. This study presents an improved method of estimating the systolic time interval over Kamoi et al. (2017), whose method did not find end systole as the dicrotic notch, but approximates it as the minimum rate of change in pressure with respect to time ($min\ dP/dt$), in the region the dicrotic notch should exist.

2. METHODS

2.1 Porcine trials and measurements

Data in this study was provided by pig experiments at the Centre Hospitalier Universitaire de Liège, Belgium. Ethics approval for the experimental procedures, protocols and use of the data was provided by the Ethics Committee of the University of Liège Medical Faculty.

Seven pure pietrain pigs weighing 20-29kg were used in the experiments, but only Pigs 2, 3, 6 and 7 are analysed. The other pigs were excluded due to differences in experimental protocol and in some places abnormalities in captured data. Pigs were administered ketamine (20 mg/kg) and diazepam (1 mg/kg) prior to the experiment. Anaesthesia was induced and maintained by continuous infu-

sion of sufentanil (0.5 μg/kg/h) and sodium pentobarbital (3 mg/kg). Pigs were intubated via tracheotomy and ventilated using a Draeger Evita2 ventilator (Draeger, Lubeck, Germany).

Pressure and volume were directly measured in the left ventricle using a 7F micromanometer-tipped admittance catheter (Transonic Sciesense Inc., Ontario, Canada) inserted into the ventricle through the right carotid artery. Pressure waveform measurements were captured at the aortic arch using 7F pressure catheters (Transonic Sciesense Inc., Ontario, Canada), inserted via the left carotid artery. All data were sampled at 1000Hz.

2.2 Hemodynamic modification

The original purpose of the experiments was to assess the accuracy of a stroke volume (SV) model (Kamoi et al., 2015). This particular model, like others, depends on accurate detection of the transition from systole to diastole. Thus, the protocols caused changes in SV, as well as significant changes in pressure waveform shape and hence dicrotic notch shape and location.

Specifically, each pig was subjected to several stepwise positive end-expiratory pressure (PEEP) recruitment manoeuvres (RM). Increases in PEEP can reduce systemic venous return to the right heart and increase pulmonary resistance. Thus, left ventricle preload decreases, leading to lower arterial pressure (Luecke and Pelosi, 2005). RMs increased PEEP in 5cmH$_2$O steps to a maximum of 15cmH$_2$O for Pig 7 and 20cmH$_2$O for Pigs 2, 3 and 6.

Experiments also included multiple fluid bolus administrations. Boluses were administered in 180ml steps ranging from 0ml to 720ml/900ml for Pigs 7/2, 3 and 6, respectively. They increased the blood volume and consequently increased atrial pressure.

Finally, experiments also involved administering a continuous dobutamine infusion to modulate contractility. Dobutamine increases contractility of the heart and can also act as a vasodialator (Ruffolo, 1987; Ellender and Skinner, 2008). It is commonly used in clinical settings to increase cardiac output (CO), driven by increased contractility (Ruffolo, 1987; Ellender and Skinner, 2008).

2.3 Data Selection Summary

The data used to test the dicrotic notch detection algorithm is taken from two distinct sections of the experiment: the *baseline* and *dobutamine high PEEP* stages. The baseline stage was when a pig was at rest following anaesthesia, but before any hemodynamic modifications were applied. Dobutamine high PEEP data was captured during the highest PEEP level of the recruitment manoeuvre that occurred during dobutamine admission. For each pig, from each stage, 10 heart beats were used, leading to a total of 80 beats for the analysis. These two stages were chosen as they represented contrasting hemodynamic states, causing significant change in the aortic pressure waveform.

2.4 Beat separation and manual dicrotic notch identification

Before dicrotic notch identification began, the start and end point were found for each beat. The feet of each waveform were found using an established algorithm discussed in detail elsewhere (Balmer et al., 2017).

To measure the accuracy of the dicrotic notch detection algorithm, the definitive dicrotic notch locations must be known. Since there is no gold standard algorithm, the best comparison is to locations chosen by trained eye, from the discrete aortic pressure signal. Therefore, points were found manually prior to the algorithm estimates. To aid in selection, the ventricular pressure waveform could be plotted with the aortic pressure signal, since after aortic valve closure, different ventricular and aortic relaxation rates lead to the divergence of the two pressure signals. This divergence served as a secondary reference for the notch location. The primary identifier being the turning point or point of inflection in the signal, following a beats maximum pressure.

2.5 Shear transform algorithm implementation

The dicrotic notch detection algorithm utilizes a shear transform. The shear line start (SP) and end points (EP), and hence gradient, are adaptive and dependent on a waveforms shape.

Both the SP and EP have separate rationales for being iterable. The aim for SP is for it to reside in the region of consistent negative pressure gradient, following the peak in the pulse pressure but prior to the dicrotic notch. EP on the other hand, is used to ensure the shear line is quasi-parallel over the region the dicrotic notch is expected to reside.

The process is as follows:

Shear line start point calculation

(1) Identify the maximum pressure in a beat (P_{max}) (example algorithm in Appendix A).
(2) Identify the point on the pressure waveform with the maximum negative (ie the minimum) gradient in a region following the P_{max} and up to a 1/3 of the time from P_{max} to the foot of the waveform. This point is labelled $P_{(min\ dP/dt)}$.
(3) Identify the point whose *pressure value* is halfway between P_{max} and $P_{(min\ dP/dt)}$ as the shear line start point (SP).
(4) Identify an initial shear line end point (EP), being a certain time between SP and the end of the current beat, based on P_{max}:
   - If $P_{max} < 100mmHg$: initial EP is 3/4 of the way from SP to end of beat.
   - If $100mmHg < P_{max} < 140mmHg$: initial EP is 1/2 of the way from SP to end of beat.
   - If $P_{max} > 140mmHg$: initial EP is 1/3 of the way from SP to end of beat.
(5) Construct the shear line over the section of pressure signal between SP and EP. Calculate the shear transform (Stevenson et al., 2012a) from the section of pressure signal to the shear line and:
   - If more than 50% of the shear transform is greater than zero, i.e. if more than 50% of the shear line is below the corresponding pressure section, assume the shear line start point was poorly identified and return to step 2, using the next most minimum gradient point to find a new SP.

- Else, assume SP has been correctly identified and move on to check and possibly update the initial EP.

Shear line end point calculation and dicrotic notch location

EP condition is based on the orthogonal distance from points on the shear line to points on the pressure waveform:

(6) Normalize the shear line and the section of pressure associated with the shear line, in both time and pressure, so that it is scale invariant.

(7) For each point on the normalized shear line, calculate the orthogonal distance to a point on the normalized pressure signal. If any point's orthogonal distance > a tolerance of 0.3, shift EP closer to SP until orthogonal distance ≤ 0.3, at which point assume EP location is adequate.

(8) Re-calculate the shear transform from the section of pressure signal, between the finalised SP and EP points, to the shear line. The point of most negative shear ($P_{min\ shear}$) is assumed to be a point in the dicrotic notch, but may not be the true minimum.

(9) Find the start of diastolic relaxation as the point of maximum pressure between the point $P_{min\ shear}$ and the end of the beat. If the dicrotic notch is a trough, this will find the local maximum turning point following the trough and is assumed the start of diastolic relaxation.

(10) Search from $P_{min\ shear}$ (inclusive) to the start of diastolic relaxation for any points lower than $P_{min\ shear}$. The lowest of these point is the estimated dicrotic notch. If there are multiple points with equal lowest values, take the middle of the lowest points as the dicrotic notch.

If P_{max} and $P_{(min\ dP/dt)}$ are close together and early enough in time, be it due to unexpected physiology or noise, there is a possibility the constructed shear line in Step 4 will be below the pressure waveform for most of its length. Hence, $P_{(min\ dP/dt)}$ is iterable, and an example is shown in Figure 1.

EP initial location being later in time for beats with low P_{max} values, is simply based on observation of later and lower pressure dicrotic notches (relative to P_{max}) in low pressure signals. However, it is possible that if EP is too late in the signal, the shear line has too lower gradient, relative to the signal, which can prove inappropriate for dicrotic notch detection, as shown in Figure 2.

2.6 Analyses

Rather than directly comparing the difference between the algorithmically determined dicrotic notch and its dicrotic notch determined by eye, the systolic time that results from each notch is compared. This is because, as discussed in the Introduction, the dicrotic notch is often found to determine systolic and diastolic time intervals (Talley et al., 1971; Payne, 2006; Marik, 2013). In addition, the shear transform method is compared with the previously published method by Kamoi et al. (2017), which, unlike the shear transform algorithm, relies on a smooth dP_{ao}/dt signal (Kamoi et al., 2017).
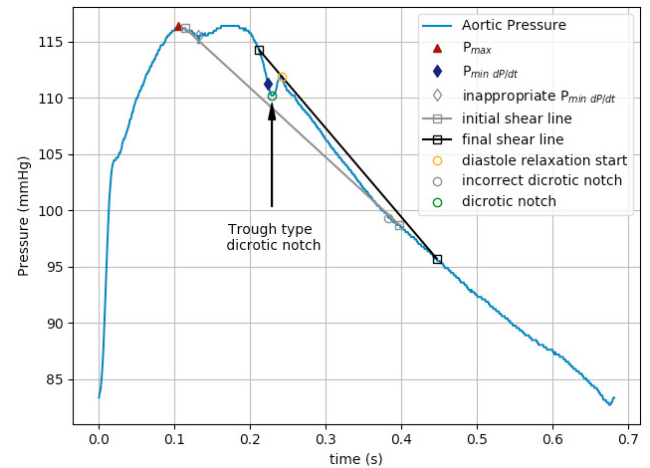

Fig. 1: The grey shear line misidentifies the dicrotic notch, due to $P_{(min\ dP/dt)}$ being too close to P_{max}. The black shear line shows the iteration of $P_{(min\ dP/dt)}$, which led to a satisfactory SP and subsequent dicrotic notch detection.
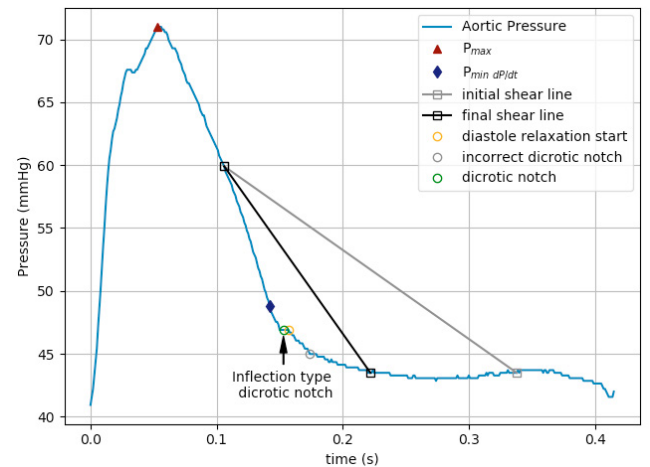

Fig. 2: The grey shear line has too greater orthogonal distance from the pressure waveform, misidentifying the dicrotic notch. The black shear line shows the iteration of EP using the orthogonality condition, and subsequent dicrotic notch detection.

The accuracy of the two algorithmic dicrotic notch detection methods (shear transform and Kamoi methods) were then analysed using two formats. Correlation plots show both the individual regression line and coefficient of determination (r^2) for each pig and data stage, as well as an overall result. The coefficient of determination, r^2, represents the fraction of the total observed variation in the algorithmically *estimated systolic time* due to the observed variation in the *measured systolic time*. The closer r^2 is to one, the better the ability of the algorithm to track changes in the measured systolic time.

Correlation however, does not imply agreement in the absolute sense (Bland and Altman, 1986). Therefore, Bland-Altman analysis was used to assess the agreement between the estimated and measured systolic time, and hence agreement between estimated and measured dicrotic notches locations.

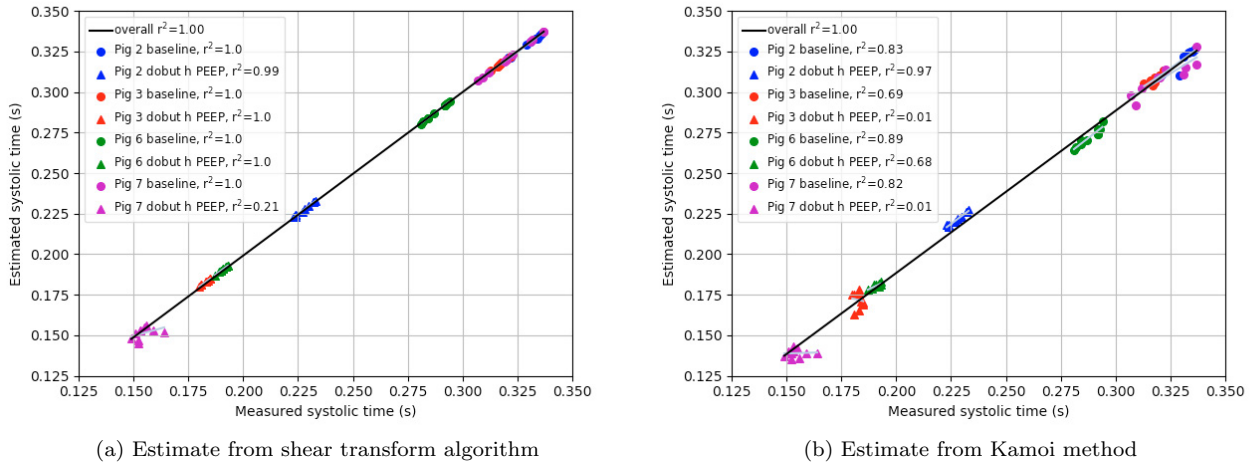(a) Estimate from shear transform algorithm

(b) Estimate from Kamoi method

Fig. 3: Regression Analysis: a) and b) show the overall and individual regression analyses for the pigs, for both the shear line estimated systolic time and Kamoi method estimated systolic time, respectively. Coefficients of determination in the legend were rounded to two decimal places and dobut h PEEP refers to the dobutamine high PEEP data.

(a) Estimate from shear transform algorithm
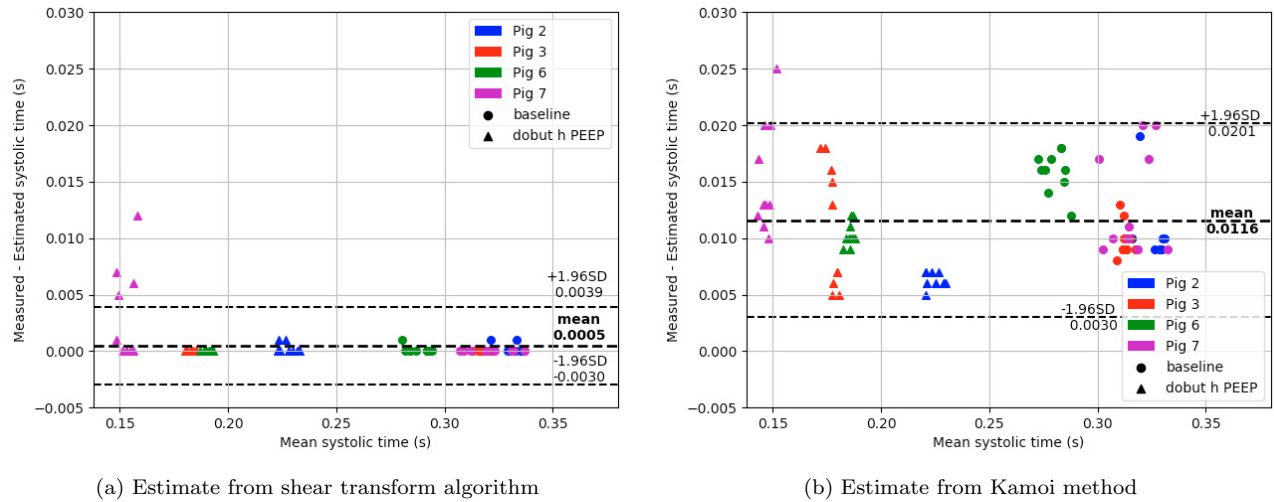

(b) Estimate from Kamoi method

Fig. 4: Bland Altman analysis: Bland Altman plots show the degree of agreement between the estimated and measured systolic times. The mean bias between the measured and estimated systolic times are shown ($\bar{d}$), as well as the limits of agreement ($\bar{d} \pm 1.96 \times SD$) to indicate the expected variation between measure and estimate. Note, dobut h PEEP label is an abbreviation of dobutamine high PEEP.

3. RESULTS & DISCUSSION

Figures 3 show the regression analysis and coefficient of determination. Bland-Altman plots are seen in Figure 4. The plots show improved trending and agreement for the shear transform algorithms over Kamoi's method.

3.1 Correlation outcomes

Figure 3 (a) & (b) show excellent overall correlations outcomes. However, the overall result alone is misleading, due the clustering of each pig's individual stage data (Bewick et al., 2003). The difference between the two algorithmic methods' ability to track changes in systolic time becomes clearer when comparing the coefficients of determination for the individual pigs and stages. In all pigs and stages, the shear transform method of dicrotic notch detection performs better than the Kamoi method,

resulting in coefficients of determination closer to 1.0. The Kamoi method's ability to track variation in systolic time reduced following hemodynamic modification, from baseline to the dobutamine high PEEP state, which is coupled with a reduction in systolic time. This is evident in the reduced coefficients of determination during dobutamine high PEEP stages. With the exception of Pig 7, the shear transform method showed no significant change in performance between hemodynamic states.

The reason for the lower performance of the Kamoi method following the hemodynamic modifications, and for the shear method in Pig 7's case, appears due to changes in the dicrotic notch shape. Taking Pigs 3 and 7 as examples: Pig's 3 dicrotic notches, in general became wider during dobutamine high PEEP ($\approx$ 28ms), compared with the baseline stage ($\approx$ 8ms), when measurements were made by eye off of the waveform plots between the widest points

of the dicrotic notches. This results in more points forming the dicrotic notch shape and hence increases the possibility that the algorithms find a point different from that chosen by eye. This is discussed further in Section 3.3. Pig 7 on the other hand, showed an almost disappearing of its dicrotic notch during dobutamine high PEEP compared to baseline, as seen in the example Figure 2. Naturally, when the dicrotic notch is difficult to detect by eye, a human observer's ability to accurately identify it is reduced. This makes it more difficult to say with certainty which dicrotic notch represents aortic valve closure best, the point identified by the algorithm or by eye. Hence in Pig 7's dobutamine high PEEP stage, poorer correlation outcome were unsurprising.

In summary, inter-pig and stage results suggest both algorithmic methods track significant changes in systolic time well. However, the tracking of the shear transform method appears superior to the Kamoi method in all cases.

3.2 Bland Altman outcomes

The contrasting systemic error of the Kamoi method relative to the shear transform method, as shown by the mean differences of $\bar{d}_{kamoi} = 11.6ms$ verses $\bar{d}_{shear} = 0.5ms$ respectively, is the most obvious result of Figure 4. Additionally, Figure 4 (b) shows the limits of agreement $(\bar{d} \pm 1.96 \times SD)$ are wider for the differences in systolic time when the Kamoi method of dicrotic notch estimation was used, 17ms vs 0.9ms for the shear transfrom detected dicrotic notches. Give that the measured systolic times ranged from 149ms to 337ms, both estimates' limits of agreement may prove to be satisfactory, however, it would depend on the specific use of the systolic time estimate. For example if the systolic time is a particularly sensitive parameter in a model, such as in Kamoi et al. (2017), the accuracy of estimation will be an important consideration.

Another interesting and obvious result, evident in both Figures 4 (a) & (b), is the bias leading to the lack of negative difference values. In the Kamoi method, this issue is easily explained: the method does not explicitly look for the dicrotic notch. Instead it applies a weighting function (WF) to the derivative of the pressure waveform with respect to time $(WF \cdot dP_{ao}/dt)$, where the weighting is applied heaviest in the region where the dicrotic notch is expected to occur. Then, the method identifies the point of most negative gradient from the weighted derivative and assumes this point is end systole/start diastole.

Because points just prior to the dicrotic notch tend to have a more negative gradient than points associated with diastolic relaxation, the Kamoi method usually finds points just prior to the dicrotic notch. The approach of using the point of most negative gradient may not make sense when a dicrotic notch is present, however, for waveforms with difficult to identify or even non-existent dicrotic notch features, the Kamoi method offers a consistent and predictable method of estimating its location, despite the early onset of diastole bias. This issue is clinically relevant given the distinct dicrotic notch shape is known to deteriorate with age (Dawber et al., 1973).

In contrast, the shear transform method is developed specifically to identify turning and inflection points of the dicrotic notch. It also never over estimated the duration of systole. A positive bias indicates the dicrotic notches identified by the shear transform method occurred before the location found by eye, and is a result of the shear transform bias discussed in the limitations section below.

3.3 Shear transform algorithm limitations

The correlation analysis in Section 3.1 revealed an increase in variation between the shear transform identified dicrotic notches and those found by eye, when a distinct turning point was not present. Secondly, the Bland-Altman analysis of Section 3.2, identified that the shear transform algorithm consistently predicted a dicrotic notch location earlier or equal too those found by eye, never later. The reason for both of these observations is evident in the way the algorithm is implemented:

The first and most obvious limitation is if the dicrotic notch depth is small or even simply flat, as it was for Pig 7's dobutamine high PEEP waveforms, it becomes difficult to identify the notches exact location. This is because the shear transform will have a similar shape to the signal from which it is derived, meaning, if no trough type notch is present in the pressure signal, none will be evident in its shear transform either.

The second less obvious impact of the dicrotic notch shape is the shear transform algorithm's bias. When the shear transform is applied, in algorithm step 8, points just left of the true dicrotic notch minimum will have a sheared value that is more negative than points just right of the minimum. In this sense, the step favours points left of the minimum to be the dicrotic notch, more than the points right of the minimum. This is because of the shear line negative gradient leading to a lower value with each time step, meaning, the vertical distance from the shear line to the dicrotic notch (the shear transform) is greatest for the points tending down into the trough of the dicrotic notch compared to a point of equal pressure but whose rising out of the trough. The same is true for cases where the dicrotic notch is in fact a flat section, or point of inflection; points left of the inflection point are favoured more than right.

The impact of this bias is most evident when algorithm steps 9 & 10 are ignored and a pressure signal with wide dicrotic notches are analysed: As previously discussed, Pig 3's dicrotic notches, in general became wider during dobutamine high PEEP ($\approx$ 28ms), compared with the baseline stage ($\approx$ 8ms). The wide dicrotic notches often had minimums with multiple points of equal pressure. Step 8 of the algorithm would find the left-most point of the minimum, while the human observer is likely to choose the middle of the multi-point minimum. Ignoring steps 9 & 10 would result in a consistent mean difference, for Pig 3's dobutamine high PEEP stage, of 3ms and range of 1ms to 7ms (results not shown). While the addition of steps 9 & 10 results in perfect dicrotic notch detection by the algorithm, with respect to those found by eye.

Thus, the accuracy of the algorithm without the final two steps is still an improvement over the Kamoi method, and may be sufficient depending on the application. However, the final steps are crucial for identifying the true dicrotic

notch minimum, thus, minimising the positive bias and maximising accuracy.

A final limitation of the study is its limited data and single location from which the pressure waveform was drawn. In the study, only 80 beats were used from two hemodynamic states and all from aortic pressure recorded in the aortic arch of pigs. While this proved adequate as a proof of concept, it would be interesting to test the algorithm on further hemodynamic states and on pressure signals common in a clinical setting, such as a femoral pressure waveform. If clinical data was used, it is also likely step 4's pressure conditions would need to be adapted to reflect hypo- and hypertension cases in humans.

4. CONCLUSION

The study aimed to develop a simple dicrotic notch detection algorithm that would improve end systole detection over an existing method. The results showed the new shear transform based detection method was better able to track changes in systolic duration and had less bias when compared with dicrotic notches manually found by eye.

REFERENCES

Balmer, J., Pretty, C., Kamoi, S., Davidson, S., Pironet, A., Desaive, T., Shaw, G.M., and Chase, J.G. (2017). Electrocardiogram R-wave is an Unreliable Indicator of Pulse Wave Initialization. In *20th IFAC World Congress 2017*. Toulouse.

Bewick, V., Cheek, L., and Ball, J. (2003). Statistics review 7: Correlation and regression. *Critical Care*, 7(6), 451–459.

Bland, J.M. and Altman, D.G. (1986). Statistical Methods for Assessing Agreement Between Two Methods of Clinical Measurement. *The Lancet*, 327(8476), 307–310.

Dawber, T.R., Thomas, H.E., and McNamara, P.M. (1973). Characteristics of the Dicrotic Notch. *Angiology*, 24(4), 244–255.

Ellender, T.J. and Skinner, J.C. (2008). The Use of Vasopressors and Inotropes in the Emergency Medical Treatment of Shock. *Emergency Medicine Clinics of North America*, 26(3), 759–786.

Hermeling, E., Reesink, K.D., Kornmann, L.M., Reneman, R.S., and Hoeks, A.P.G. (2009). The dicrotic notch as alternative time-reference point to measure local pulse wave velocity in the carotid artery by means of ultrasonography. *Journal of Hypertension*, 27(10).

Kamoi, S., Pretty, C., Balmer, J., Davidson, S., Pironet, A., Desaive, T., Shaw, G.M., and Chase, J.G. (2017). Improved pressure contour analysis for estimating cardiac stroke volume using pulse wave velocity measurement. *BioMedical Engineering OnLine*, 16(1), 51.

Kamoi, S., Pretty, C., Chiew, Y.S., Davidson, S., Pironet, A., Desaive, T., Shaw, G.M., and Chase, J.G. (2015). Relationship between stroke volume and pulse wave velocity. *IFAC-PapersOnLine*, 28(20), 285–290.

Lewis, T. (1906). The factors influencing the prominence of the dicrotic wave. *J. of Physiology*, 34(6), 414–429.

Luecke, T. and Pelosi, P. (2005). Clinical review: Positive end-expiratory pressure and cardiac output. *Critical Care*, 9(6), 607–621.

Marik, P.E. (2013). Noninvasive cardiac output monitors: A state-of the-art review. *Journal of Cardiothoracic and Vascular Anesthesia*, 27(1), 121–134.

Oppenheim, M.I. and Sittig, D.F. (1995). An innovative dicrotic notch detection algorithm which combines rule-based logic with digital signal processing techniques. *Computers and biomedical research, an international journal*, 28(2), 154–170.

Payne, R.A. (2006). Pulse transit time measured from the ECG: an unreliable marker of beat-to-beat blood pressure. *J. of Applied Physiology*, 100(1), 136–141.

Ruffolo, R.R. (1987). Review: The Pharmacology of Dobutamine. *The American Journal of the Medical Sciences*, 294(4), 244–248.

Stevenson, D., Revie, J., Chase, J.G., Hann, C.E., Shaw, G.M., Lambermont, B., Ghuysen, A., Kolh, P., and Desaive, T. (2012a). Algorithmic processing of pressure waveforms to facilitate estimation of cardiac elastance. *Biomedical engineering online*, 11, 28.

Stevenson, D., Revie, J., Chase, J.G., Hann, C.E., Shaw, G.M., Lambermont, B., Ghuysen, A., Kolh, P., and Desaive, T. (2012b). Beat-to-beat estimation of the continuous left and right cardiac elastance from metrics commonly available in clinical settings. *Biomedical engineering online*, 11, 73.

Stevenson, D., Hann, C., Chase, G., Revie, J., Shaw, G., Desaive, T., Lambermont, B., Ghuysen, A., Kolh, P., and Heldmann, S. (2010). Estimating the driver function of a cardiovascular system model. *IET Seminar Digest*, 2010.

Talley, R.C., Meyer, J.F., and McNay, J.L. (1971). Evaluation of the pre-ejection period as an estimate of myocardial contractility in dogs. *The American Journal of Cardiology*, 27(4), 384–391.

Appendix A. MAXIMUM PRESSURE ALGORITHM

(1) In a signal containing multiple beats, calculate a central moving average such that gradual changes in pressure are captured.

(2) Identify where the moving average *crosses* the pressure signal.

(3) Provided the central moving average used sufficient points, between intercepts i & $(i+2)$, (i.e. an intercept and its neighbours neighbour forward in time), a minimum & maximum should reside.
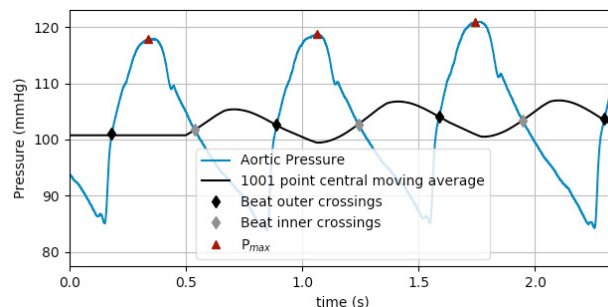

Fig. A.1: Max pressure algorithm example waveform. Note the initial condition utilizing a fix mean for the first 500 points before central moving average is implemented.